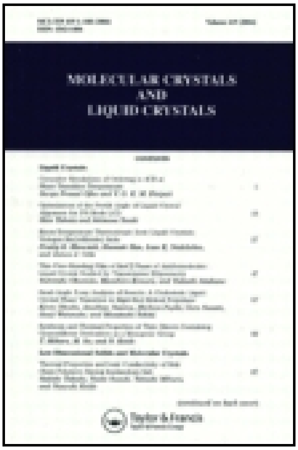

Molecular Crystals and Liquid Crystals Science and Technology. Section A. Molecular Crystals and Liquid Crystals

Publication details, including instructions for authors and subscription information:
http://www.tandfonline.com/loi/gmcl19

A Novel Spin Wave from Low-Dimensional Superlattice of Microstructured Ferromagnetic Thin Films

Ko Furukawa [a], Daisuke Shiomi [a], Kazunobu Sato [a], Takeji Takui [a], Koichi Itoh [a], Atsushi Maeda [b], Minoru Kume [b], Kenichi Shibata [b] & Isao Nakatani [c]

[a] Departments of Chemistry and Material Science, Graduate School of Science, Osaka City University, Osaka, 558-8585, Japan

[b] SANYO Electric Co., Ltd., Moriguchi, 570-0016, Japan

[c] National Research Institute for Metals, Tsukuba, 305-0047, Japan

Version of record first published: 24 Sep 2006

Mol. Cryst. and Liq. Cryst., 1999, Vol. 335, pp. 163-172
Reprints available directly from the publisher
Photocopying permitted by license only

A Novel Spin Wave from Low-Dimensional Superlattice of Microstructured Ferromagnetic Thin Films

KO FURUKAWA[a], DAISUKE SHIOMI[a], KAZUNOBU SATO[a], TAKEJI TAKUI[a], KOICHI ITOH[a], ATSUSHI MAEDA[b], MINORU KUME[b], KENICHI SHIBATA[b] and ISAO NAKATANI[c]

[a]*Departments of Chemistry and Material Science, Graduate School of Science, Osaka City University, Osaka 558–8585, Japan,* [b]*SANYO Electric Co., Ltd., Moriguchi 570–0016, Japan and* [c]*National Research Institute for Metals, Tsukuba 305–0047, Japan*

We examined the dynamical magnetic properties of microstructured ferromagnetic thin films with low-dimensional superlattice structure by ferromagnetic resonance (FMR) spectroscopy. The superlattice is composed of one- or two-dimensional arrays of "islands" of permalloy on micron scale. The conventional standing spin wave (SSW) model couldn't reproduce the angular variation of the observed FMR spectra. We analyzed the observed FMR spectra by the dipolar spin wave (dipolar SW) model describing collective motion of gigantic magnetic moments, which are defined by a whole magnetization of the semimacroscopic-scale "island". From the analysis of the observed angular variation, the dispersion relation for the dipolar SW was found to be the general formulation for the dynamical magnetic properties of the semimacroscopic systems. It was found from the analysis of the distance dependence of the inter-island magnetic interactions that the size and the shape of the ferromagnetic islands are not negligible in the dipolar SW.

Keywords: microstructured thin film; permalloy; ferromagnetic resonance; dipolar spin wave; superlattice; semimacroscopic magnetic system

INTRODUCTION

Spin-dependent transport properties such as spin-polarized tunneling phenomena[1] and magneto-resistance[2] in artificially structured materials have received considerable attention. We have reported another type of novel magnetic functionality in materials with superlattice structure[3-5]: A spin wave-like collective motion arising from magnetic dipolar interactions has been found in microstructured thin films of ferromagnetic materials[3-5]. The collective motion has been termed as "dipolar spin wave" (dipolar SW).

In the present study, we examine the validity and limitation of the magnetic dipolar SW model by ferromagnetic resonance (FMR) spectroscopy. Figure 1 shows the microstructured thin films under study in which the micron-scale "islands" of ferromagnetic permalloy ($Fe_{20}Ni_{80}$) are aligned to make one-dimensional (1-d) "stripe-array" and two-dimensional (2-d) "box-array" on the Si substrates. The dipolar SW has been regarded as a collective motion of gigantic magnetizations of the islands[3-5]. We illustrate that the dipolar SW model is validated both in the 1-d and 2-d systems with various kinds of spatial geometry on the basis of a common formulation. The limitation of the dipolar SW model is elucidated by analyzing inter-island distance dependence of the dipolar interactions. Group-theoretical symmetry property appearing in the FMR spectra is also discussed in the light of a shape effect inherent in the finite-size magnetization, which is characteristic of the semimacroscopic systems.

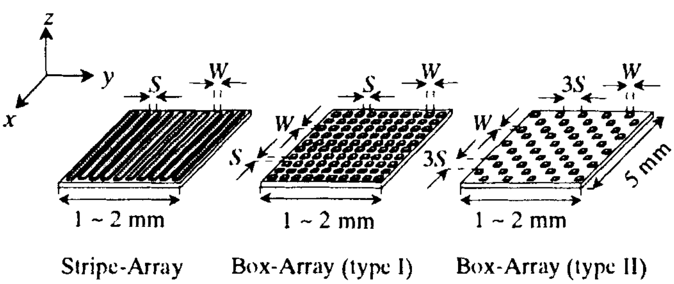

FIGURE 1 The microstructured thin films of ferromagnetic permalloy ($Fe_{20}Ni_{80}$). The inter-island distance S and the width of the island W are ranging from 1.0 to 2.0 μm. The xyz coordinate system is fixed in the thin films.

EXPERIMENTAL

The thin films were fabricated by the electron-beam lithography[6, 7]. The films are 50nm in thickness. The *xyz*-coordinate system is fixed in the thin films. The FMR spectra were recorded on a Bruker ESP300 spectrometer (X-band, TM mode cavity) at room temperature.

RESULTS AND DISCUSSION

The Dipolar Spin Wave Model

Figure 2 shows one of the FMR spectra observed for the 1-d and 2-d arrays with the external magnetic field $\boldsymbol{B}_0$ along the *y*-axis. The conventional standing SW (SSW) model[8] was not valid for interpreting the observed FMR spectra for the following two reasons: (I) The satellite peaks with weak intensity appeared at higher field than the main peak with the largest intensity, while for the conventional SSW, a series of satellite signals attributable to FMR of the SSW mode should appear at lower field than the main FMR signal from the uniform precession mode. (II) Satellite signals up to the 6-th order were observed. Considering the thickness of the film, the number of the satellite signals for the observed FMR spectra exceeds that for the conventional SSW. The conventional SSW model fails to explain the observed FMR spectra.

Let us summarize here the picture of the dipolar SW[3-5]. A whole magnetization of the ferromagnetic island is regarded as a gigantic magnetic moment, which is coupled with those of neighboring islands by magnetic

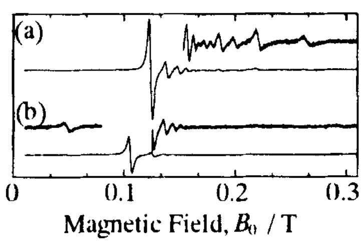

FIGURE 2 The observed FMR spectra for (a) the 1-d stripe-array ($S = W = 1.5$ μm) and (b) the 2-d box-array (Type I, $S = W = 1.0$ μm) with $\boldsymbol{B}_0 // y$.

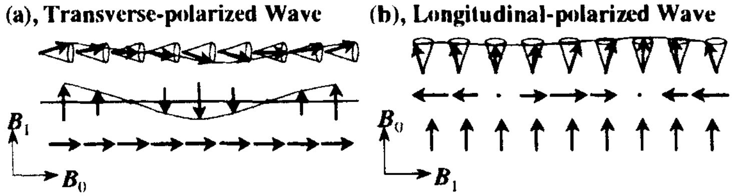

FIGURE 3 The schematic views of the dipolar SW for the 1-d stripe-array (a: The transverse-polarized wave under $\boldsymbol{B}_0$ // y and $\boldsymbol{B}_1$ // z; b: The longitudinal-polarized wave under $\boldsymbol{B}_0$ // z and $\boldsymbol{B}_1$ // y). The arrow with cone in the upper figures denotes the precessing magnetization $\boldsymbol{M}$ of the island. In the lower portions are drawn the dynamical (// $\boldsymbol{B}_1$) and the static components (// $\boldsymbol{B}_0$) of $\boldsymbol{M}$.

dipolar interactions. A spin wave-like collective excitation of the moments is expected to occur, when the static magnetic field and the microwave-oscillating field are applied. As an illustration, the dipolar SW in the 1-d stripe-array is shown in Fig.3. When the static field $\boldsymbol{B}_0$ is applied along the y direction and $\boldsymbol{B}_1$ along the z direction, the transverse-polarized wave of the gigantic magnetic moments is excited (Fig. 3a). The dynamical (//$\boldsymbol{B}_1$) and the static component (//$\boldsymbol{B}_0$) of the transverse wave are shown in the lower portions of Fig. 3. For $\boldsymbol{B}_0$ // z and $\boldsymbol{B}_1$ // y, the longitudinal-polarized wave of the magnetic moments is excited (Fig. 3b).

The equation of motion for the magnetization $\boldsymbol{M}$ of the island is expressed as

$$\frac{d\boldsymbol{M}}{dt} = \gamma\left[\boldsymbol{M} \times \left(\boldsymbol{B}_0 + \boldsymbol{B}_1 + \boldsymbol{B}_{\mathrm{dip}}\right)\right], \tag{1}$$

where γ is the gyromagnetic ratio, $\boldsymbol{B}_1$ the oscillating field of the microwave and $\boldsymbol{B}_{\mathrm{dip}}$ the mean dipolar field. The demagnetization field is included in $\boldsymbol{B}_{\mathrm{dip}}$. Since we don't discuss the line width and the line shape of the spectra, the relaxation term is ignored in Eq.(1). The dispersion relations of the dipolar SW are derived from Eq.(1) for the 1-d and 2-d arrays. The geometrical symmetry of microstructure is reflected in the mean dipolar field $\boldsymbol{B}_{\mathrm{dip}}$ as described below.

The magnetization vector $\boldsymbol{M}$ is not always parallel to the external static field $\boldsymbol{B}_0$ owing to the anisotropic demagnetization field [9-11]. Therefore, we must consider an additional coordinate system, the *XYZ*-coordinate system, in which the direction of the precession axis of the gigantic magnetic moment $\boldsymbol{M}$ is defined as collinear to the *Z*-axis. The *XYZ* system is related to the *xyz* system by a unitary transformation matrix $\boldsymbol{U}$, $\boldsymbol{U}\boldsymbol{r}^{(XYZ)} = \boldsymbol{r}^{(xyz)}$. When $\boldsymbol{B}_0$ is applied along one of the principal directions (x, y, or z), $\boldsymbol{M}$ is collinear to $\boldsymbol{B}_0$.

The effective mean-dipolar field $\boldsymbol{B}_{\rm dip}$ is expressed by the sum of the following two kinds of contributions; (i) $\boldsymbol{B}^k_{\rm dip}$: the dynamical term from the precessing $\boldsymbol{M}$ (M_X and M_Y) and (ii) $\boldsymbol{B}^0_{\rm dip}$: the static term from M_Z. The mean dipolar fields $\boldsymbol{B}^k_{\rm dip}$ and $\boldsymbol{B}^0_{\rm dip}$ are expressed as follows;

$$\boldsymbol{B}^k_{\rm dip} = \boldsymbol{T}^k \boldsymbol{M}^k, \tag{2}$$

$$\tilde{\boldsymbol{M}}^k \equiv (M_X, M_Y, 0) = (M_{XY}\exp[\,j(\boldsymbol{k}\cdot\boldsymbol{r} - \omega t)], M_{XY}\exp[\,j(\boldsymbol{k}\cdot\boldsymbol{r} - \omega t)], 0), \tag{3}$$

and

$$\boldsymbol{B}^0_{\rm dip} = \boldsymbol{T}^0 \boldsymbol{M}^0, \tag{4}$$

$$\tilde{\boldsymbol{M}}^0 \equiv (0, 0, M_Z) \qquad (M_Z \approx M \equiv |\boldsymbol{M}|), \tag{5}$$

where $\boldsymbol{T}^k$ and $\boldsymbol{T}^0$ stand for the dipolar interaction. $\boldsymbol{k}$ and $\boldsymbol{r}$ in $\tilde{\boldsymbol{M}}^k$ represent the wave vector and the primitive translational vector of the wave, respectively. The dispersion relation for the dipolar SW is derived from Eqs. (1)–(5);

$$(\omega/\gamma)^2 = \left[B_{0Z} + \left(T^0_{ZZ} - T^0_{XX} - T^k_{XX}\right)M\right] \times \left[B_{0Z} + \left(T^0_{ZZ} - T^0_{YY} - T^k_{YY}\right)M\right] - \left(T^0_{XY} + T^k_{XY}\right)^2 M^2. \tag{6}$$

<u>**Angular Dependence of the Resonance Field for 1-d Stripe-Array**</u>

The angular dependence of the observed resonance field for the 1-d stripe array is depicted in Fig.4. In applying the dipolar SW model to the 1-d array, the dipolar interaction tensors $\boldsymbol{T}^k$ or $\boldsymbol{T}^0$ are expressed as

$$\boldsymbol{T}^k = \boldsymbol{U}^{-1}\begin{pmatrix} 0 & 0 & 0 \\ 0 & Dk & 0 \\ 0 & 0 & Ek \end{pmatrix}\boldsymbol{U}, \tag{7}$$

$$T^{0} = U^{-1}\begin{pmatrix} 0 & 0 & 0 \\ 0 & D_0 - N_y & 0 \\ 0 & 0 & E_0 - N_z \end{pmatrix} U, \tag{8}$$

on the basis of the geometrical symmetry of the microstructure. The parameters D, E, D_0, and E_0 stand for the dipolar interactions between the islands and N_y and N_z for the demagnetization. After substituting Eqs.(7) and (8) into Eq.(6), Eq. (6) was least-square fitted to the observed resonance field. The resonance fields calculated from Eq. (6) are shown in Fig. 4 as a function of the orientation of $\boldsymbol{B}_0$. The fit to the observed resonance fields is satisfactory. For another film with finer superstructure (S = W = 1.0 μm), a similar fit has been obtained. The optimized parameters for the 1-d stripe-arrays are summarized in Table I. The observed FMR spectra have been reproduced by the calculations based on the dipolar SW model.

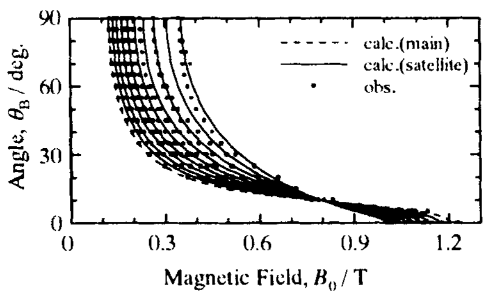

FIGURE 4 The angular dependence of the resonance fields for the stripe-array (S = W = 1.5 μm). The angle θ = 0 defines the field $\boldsymbol{B}_0$ parallel to the z-axis. The broken line stands for the calculated value of the main signal, the solid lines for the calculated values of the satellite signals and the dots for the observed values.

TABLE I Fitting parameters for the 1-d stripe-arrays.

S, W / μm	D_0-N_y / 10^{13}m^{-3}	E_0-N_z / 10^{16}m^{-3}	D / 10^{12}m^{-2}	E / 10^{12}m^{-2}	M / 10^{-10} Am^2
1.0	-0.999	-3.48	-0.158	0.219	2.05
1.5	-3.18	-0.234	-0.792	0.290	3.07

Angular Dependence of the Resonance Field for 2-d Box-Array

The angular dependence of the observed resonance field for the 2-d box array is shown in Fig. 5. We assume that a two-dimensional dipolar SW is excited in the 2-d box-array, which is described well by the linear combination of independent plane waves. In analyzing the observed spectra on the basis of the dipolar SW model which has succeeded in describing the 1-d dipolar SW, we modify only the interaction tensors $\boldsymbol{T}^k$ and $\boldsymbol{T}^0$ as follows

$$\boldsymbol{T}^k = \boldsymbol{U}^{-1}\begin{pmatrix} D_x k_x + D_y k_y & 0 & 0 \\ 0 & E_x k_x + E_y k_y & 0 \\ 0 & 0 & E_x k_x + E_y k_y \end{pmatrix}\boldsymbol{U}, \tag{9}$$

and

$$\boldsymbol{T}^0 = \boldsymbol{U}^{-1}\begin{pmatrix} D_0 - N_x & 0 & 0 \\ 0 & E_0 - N_y & 0 \\ 0 & 0 & E_0 - N_z \end{pmatrix}\boldsymbol{U}, \tag{10}$$

where D_0, E_0, D_x, D_y, E_x and E_y stand for the dipolar interaction parameters, N_x, N_y and N_z for the demagnetization factors. k_x and k_y are the wave number in the x and y directions, respectively. Substituting Eqs (9) and (10) into Eq. (6) and Eq. (6) is least-square fitted to the observed resonance fields for the

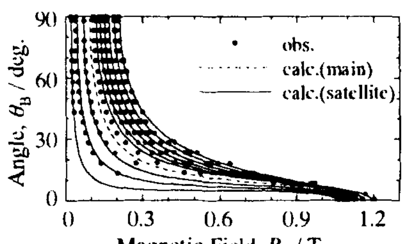

FIGURE 5 The angular dependence of the resonance fields for the box-array (Type I, $S = W = 1.0$ μm). The angle $\theta = 0$ defines the field $\boldsymbol{B}_0$ parallel to the z-axis. The broken line stands for calculated value of the main signal, the solid lines for the calculated values of the satellite peaks and the dots for the observed values.

box-array (Type I, $S = W = 1.0$ μm). The calculated angular dependence of the resonance fields in the yz-plane is in agreement with the observed ones as shown in Fig. 5. For all the other films under study (Type I, $S = W = 1.5$ μm; Type II, $S = W = 1.0$, 1.5, 2.0 μm), good fits have been obtained. The optimized parameters are summarized in Table II.

TABLE II Fitting parameters for 2-d box-array

Type, S, W / μm	D_0-N_y / 10^{19} m^{-3}	E_0-N_z / 10^{19} m^{-3}	D_x / 10^{14} m^{-2}	D_y / 10^{14} m^{-2}	E_x / 10^{15} m^{-2}	E_y / 10^{15} m^{-2}	M / 10^{-14} Am^2
I, 1.0	0.553	-1.10	-6.78	3.39	-1.27	-1.27	4.09
I, 1.5	0.252	-0.504	-1.82	0.908	-0.387	-0.387	9.21
II, 1.0	0.559	-1.12	-6.64	3.32	-1.25	-1.25	4.09
II, 1.5	0.256	-0.511	-1.94	0.968	-0.397	-0.397	9.21
II, 2.0	0.143	-0.285	-0.846	0.423	-0.168	-0.168	17.6

The dipolar SW model, Eqs.(1)-(6), succeeded in reproducing the observed FMR spectra both from the 1-d stripe arrays and 2-d box-arrays. Only the diagonal elements of the dipolar interaction tensors were modified to apply the model to two kinds of systems with different types of geometry and dimensionality. It has been found that Eqs.(1)-(6) of the dipolar SW model is a general formulation which is valid for describing the dynamical magnetic properties of low-dimensional microstructured thin films with various superlattice structures.

The Shape Effect in the Semimacroscopic Systems

In order to clarify the validity and limitation of the dipolar SW model, the inter-island distance dependence of the dipolar interaction parameters are examined. Figure 6a shows the dipolar parameter D_0–N_y for Type I and II of the box-arrays as a function of the distance, δ (Type I: $\delta = 2S = 2W$, Type II: $\delta = 2\sqrt{2}\,S = 2\sqrt{2}\,W$), between the center of the nearest neighbor islands. If the point dipole approximation is valid for the dipolar interactions between the islands in the semimacroscopic systems and the nearest-neighbor interactions are dominant, the dipolar interaction parameters should be proportional to $1 / \delta^3$ and the distance dependence for Type I should coincide with that for Type II. As shown in Fig.6, the distance dependence for Type

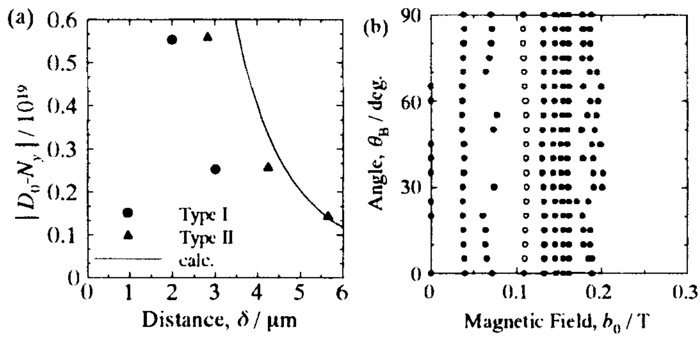

FIGURE 6 (a) The distance dependence of the dipolar parameter (D_0 - N_y) for the box-array (circles: Type I; triangles: Type II). The solid line represents $|D_0$-$N_y|$ prop. $1/\delta^3$. (b) Angular dependence of the resonance filed for the box-array (Type I, $S = W = 1.0$ μm) in the xy plane. The open circles stand for the main signals and the closed circles for the satellite signals.

II shows departure from the $1/\delta^3$-curve and doesn't agree with that for Type I, revealing the breakdown of the point dipole approximation: the size and the shape of the ferromagnetic island is not negligible.

The box-arrays seem to have tetragonal symmetry. If the group-theoretical symmetry property holds for the semimacroscopic system, a tetragonal degeneracy should appear; angular dependence of the resonance field in the xy-plane of the 2-d box-array should vanish. Figure 6b shows the resonance field for the 2-d box-array (Type I, $S = W = 1.0$ μm) as a function of the direction of the applied field $\boldsymbol{B}_0$ in the xy plane. The resonance field for the box-array depends on the angle, θ_B. Departure from the group-theoretical degeneracy in microscopic terms found in the in-plane spectra is possibly related to the breakdown of the point-dipole treatment.

CONCLUSION

We have measured the FMR spectra from the 1-d and 2-d microstructured ferromagnetic thin films and the spectra have been interpreted by the magnetic dipolar SW model. The magnetic dipolar SW model is valid for reproducing the FMR spectra from both the 1-d and 2-d arrays with various S and W values (1.0 μm < S, W < 2.0 μm), and has been given a rationale by the dispersion relation, Eq. (6), for the superlattice systems. The extension of the model to the 2-d systems has involved the assumption that the 2-d dipolar SW can be described well by the linear combination of the independent plane waves. For verifying thoroughly the validity of the assumption, thin films with other geometries and sizes should be studied.

From the analysis of the principal values of the dipolar interaction tensors, it has been found that the point-dipole treatment was not applicable. The dipolar parameters obtained from the analysis indicate the shape effect. This reflects a characteristic of the semimacroscopic magnetic systems.

References

[1] For example, see, M.N. Baibich, J.M. Broto, A. Fert, F. Nguyen Van Dau, F. Petroff, P. Eitenne, G. Creuzet, A. Friederich, and J. Chazelas, *Phys. Rev. Lett.*, **61,** 2471(1988).
[2] For example, see, P.M. Tedrow, and R. Meservey, *Phys. Rev. Lett.*, **26,**192(1971).
[3] D. Shiomi, K. Furukawa, K. Sato, T. Takui, K. Itoh, A. Maeda, S. Takahashi, and I. Nakatani, *Phys. Rev. Lett.*, Submitted.
[4] K. Furukawa, D. Shiomi, K. Sato, T. Takui, K. Itoh, A. Maeda, M. Kume, K. Shibata, and I. Nakatani, *Magnetic Resonance and related phenomena vol. II,;* Proceedings of the Joint 29th AMPERE – 13thISMAR International Conference, edited by D. Ziessow, W. Lubitz, and F. Lendzian (Berlin, 1998), P. 1033.
[5] K. Furukawa, D. Shiomi, K. Sato, T. Takui, K. Itoh, A. Maeda, M. Kume, K. Shibata, and I. Nakatani, *Syn. Met.*, Submitted.
[6] I. Nakatani, *IEEE Trans. Magn.*, **32,** 4448 (1996).
[7] A. Maeda, M. Kume, T. Ogura, and K. Kuroki, *J. Mag. Soc. Japan,* **19,**309 (1995); **19,** 397 (1995); **19,** 831 (1995).
[8] C. Kittel, *Phys. Rev.,* **110,**1295 (1958).
[9] M. Okochi, and H. Nose, *J. Phys. Soc. Japan,* **27,** 312 (1969).
[10] R.F. Soohoo, *Phys. Rev.,* **131,** 594 (1963).
[11] T. Oguchi, *Prog. Theo. Phys.,* **17,** 659 (1957).